Microfluidic fabrication of microcapsules tailored for self-healing in cementitious materials
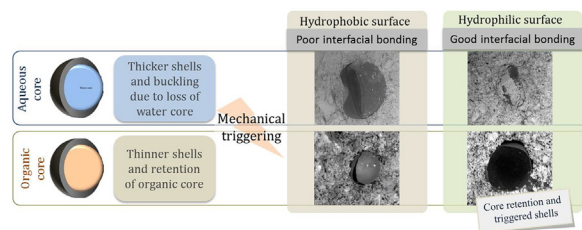
Lívia Souza *, Abir Al-Tabbaa

Department of Engineering, University of Cambridge, Trumpington Road, Cambridge CB2 1PZ, UK

HIGHLIGHTS

- Aqueous and organic core were encapsulated using microfluidics.
- Retention of colloidal silica and organic phase was demonstrated.
- Microcapsules were functionalised to increase shell-matrix interfacial bonding.
- Core retention and hydrophilic surface facilitated physical triggering.

GRAPHICAL ABSTRACT

ARTICLE INFO

ABSTRACT

Autonomic self-healing in cement-based infrastructure materials has recently emerged as a promising strategy for extending the service life of concrete infrastructure. Amongst the various self-healing systems being developed, the use of microcapsules has received significant attention partly because of its ease implementation. Up to date, microcapsules for self-healing applications have been mainly manufactured using bulk emulsifications polymerisation techniques. However this methodology raises concerns regarding shell dimensions and interfacial bonding. This study proposes for the first time the fabrication of microcapsules with tailored characteristics for mechanically triggered self-healing action in cement-based composites. For this, a microfluidic device was used to produce a double emulsion template for the formation of microcapsules, containing both aqueous and organic liquid core. In addition, a novel method has been proposed to functionalize the microcapsules' surface with hydrophilic groups in order to increase the interfacial bond with the cementitious host matrix. The core retention was studied using EDX and TGA, and their mechanical triggering was investigated via SEM of the microcapsules embedded in the cement paste. The results demonstrated the capability of microfluidics to produce microcapsules with liquid organic core, thin shell, hydrophilic surface and appropriate fracture strength for use in mechanically triggered self-healing of cementitious materials.

1. Introduction

Under service conditions, concrete structural elements develop microcracks which, with continuous environmental and mechanical loading, have the tendency to coalesce and form larger cracks. The latter create a preferential pathway for aggressive species (e.g. oxygen, CO_2, chloride ions, sulphates) to penetrate the con-crete, reducing its alkalinity and generating fertile conditions for steel corrosion to initiate. The construction codes of practice generally treat material and structural degradation as inevitable events. The long-term material behaviour is largely overlooked and structural weathering is treated using expensive maintenance regimes. In the UK alone, repair and maintenance actions resulted in a cost of ∼£50 billion/year [1]. In the United States, the cost for repair, rehabilitation, strengthening and protection of the concrete structures was estimated between $18 and $21 billion/year [2]. In addition, the associated costs for maintenance due to steel corrosion

reach $23 billion/year in the U.S. only [3,4]. Furthermore, indirect costs due to traffic jams and loss of productivity calculated through life cycle analyses can be more than 10 times the direct cost of maintenance and repair [5,6].

To overcome the limitations associated with crack propagation and maintenance actions, the concept of self-healing has emerged [7,8]. For self-healing, the formation of cracks is not problematic as long as it is counteracted by an autonomous process of healing the damage [9]. In other words, it relies on a self-initiated response of the system to detect and recover autonomously, without external interaction. A promising approach to achieve self-healing is the addition, during the mixing process, of microcapsules containing healing agent. Upon triggering, the shell releases the healing agent and the crack is then repaired, as shown schematically in Fig. 1. Capsule-based self-healing have been reported to successfully heal cracks up to 1 mm [10].

For this mechanically triggered self-healing, several microencapsulation techniques have been explored to produce aqueous or organic core materials, such as coacervation [11,12], in-situ polymerization [10,13–15] and sol-gel [16]. These liquid cores include organic precursor for polymeric healing [15–17], bacterial spores suspended in organic substrate [10] and mineral healing agents [11–13,18,19]. However, the interfacial bonding between the shell and the cementitious materials is a concern, since it may lead to debonding of the capsules instead of rupture [20]. In general, a good interfacial bonding between a polymeric material and the cementitious matrix is ensured by the presence of hydrophilic groups, which are compatible with the water-based cementitious matrix [21–24]. In contrast, the formation of poly(urea-formaldehyde) (PUF) shell, for example, relies on the deposition of water-insoluble prepolymer in the oil/water interface which ultimately becomes highly cross-linked forming and encapsulating the core material [25]. Despite the presence of the hydroxyl, amino and carboxyl polar groups in the PUF shell, the interfacial bonding with the cementitious matrix may not be efficient and debonding has been observed [15]. Likewise, shell prepared with non-polar phenol-formaldehyde groups results in poor interfacial bonding and may debond upon crack formation [17]. Alternatively, coacervation and sol-gel reactions offer alternative routes to the production of microcapsules with compatible shell to promote the interfacial bonding via chemical reactions. This was confirmed by elemental analysis of the interface between the gelatine microcapsules, showing the presence of ettringite and calcium silicate hydrates (C-S-H) [18]. Similarly, EDX analysis suggested a chemical

reaction between the silica capsules' shell with the matrix, resulting in a tight interface [26]. However, conventional bulky emulsification methodologies typically produce microcapsules with a wide range of sizes and shell thicknesses. Since the physical triggering is based on the dimensions of the shell, the variety of size and shell thickness results in poor control of the release of the healing agent.

Although still unexplored for self-healing of cementitious materials, microfluidic encapsulation is a resourceful tool to produce monodisperse capsules with precise control over the core/shell ratio and high encapsulation efficiency [27,28]. Using the double emulsion template, a wide variety of shell materials can be explored, and the properties can be modulated to fine-tune payload, permeability and shell properties of the microcapsules [29,30]. The technique has also been reported to encapsulate materials with potential to be used as healing agent, such as such as amines for polymeric healing [27], biological cargo [31] and mineral agents [32]. Thus, this effective platform to produce core-shell structures can be used to investigate the importance of core retention and the interfacial bonding for physical triggering.

This work explores the microfluidic approach for production of microcapsules with polymeric shells encapsulating compounds for self-healing action in cementitious materials. Aqueous and non-aqueous compounds were encapsulated by an acrylate shell producing monodisperse microcapsules. The retention of colloidal silica, a mineral healing agent, and mineral oil within the resultant microcapsule is demonstrated using energy dispersive X-ray analysis (EDX) and thermogravimetric analysis. To enhance the interfacial bonding between the microcapsules and the cementitious matrix, the acrylate shell was functionalised with carboxylic groups which increase the hydrophilic nature of the shell. In addition, glass transition temperature, Young's modulus and tensile strength of the acrylate shell used of the production of the microcapsules, were investigated with respect to their compliance with the host matrix. The research focuses on the potential of this controlled emulsification process as a technique to generate microcapsules for the systematic investigation of capsule-based self-healing cement-based materials.

2. Materials and methods

2.1. Production of microcapsules

A complete set up of the microfluidics system is shown in Fig. 2a [33]. To produce the double emulsion template, a flow-focusing microfluidic device (Dolomite Microfluidics, UK) was used, as shown in Fig. 2c, d. In this emulsion, the compound to be encapsulated formed the inner phase whereas the polymeric shell, which was a photocurable oil, formed the outer phase. The former was injected through the capillary tube, while the photocurable oil (dispersed phase) was pumped through the central channel and the continuous phase flowed in the two side channels (Fig. 2d). The fluids met at the cross-junction, forming jets of the dispersed phase containing the inner phase as the fluids streamed into the main outlet channel. The fluids were injected using pressure pumps (Dolomite Microfluidics, UK) at typical flow rates of 2–6 µL/min, 2–7 µL/min and 50–80 µL/min for the inner, middle and outer fluids, respectively. For the aqueous core microcapsules, the double emulsion of water-in-oil-in-water (w/o/w) was formed with an inner aqueous solution that contained 5 wt% poly(vinyl alcohol) (PVA, MW 31000–50000, 98–98.8% hydrolyzed, Acros Organics) and 50 wt% colloidal silica (LUDOX HS-40, 40 wt% colloidal silica suspension in water, Sigma Aldrich). For the organic core microcapsules, the double emulsion of oil-in-oil-in-water (o/o/w) was formed with an inner fluid containing a mineral oil phase (light mineral oil, Sigma Aldrich). For the middle phase, two solutions were produced, BH and BI. The former, comprised of 50 wt% 1,6-hexanediol diacrylate (HDDA, Sigma Aldrich) and 50 wt% bisphenol A glycerolate dimethacrylate (BisGMA, Sigma Aldrich) whereas BI solution consisted of 50 wt% isobornyl acrylate (IBOA, Sigma Aldrich) and 50 wt% BisGMA. The solutions were mixed using a magnetic stirrer until a homogenous solution was achieved and followed by the addition of 1 wt% of photoinitiator hydroxy-2-methylpropiophenone (Sigma Aldrich). As outer fluid, 2 wt% aqueous solutions of PVA was used. To functionalise the surface of the microcapsules, an aqueous solution consisting of 5 wt% PVA and 1 wt% of acrylic acid (Sigma Aldrich) was used as outer fluid. The polymerisation of the shell took place using a UV-lamp (Sylvania, BL350) exposed over the collection tube shortly (Fig. 2b) after the formation of the double emulsion droplets
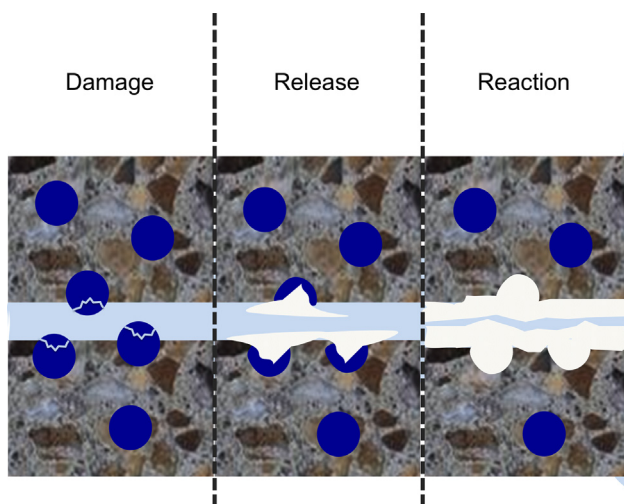

Fig. 1. Schematic of mechanically triggered capsule-based self-healing in cementitious matrix (Credit: Dr. Chrysoula Litina).
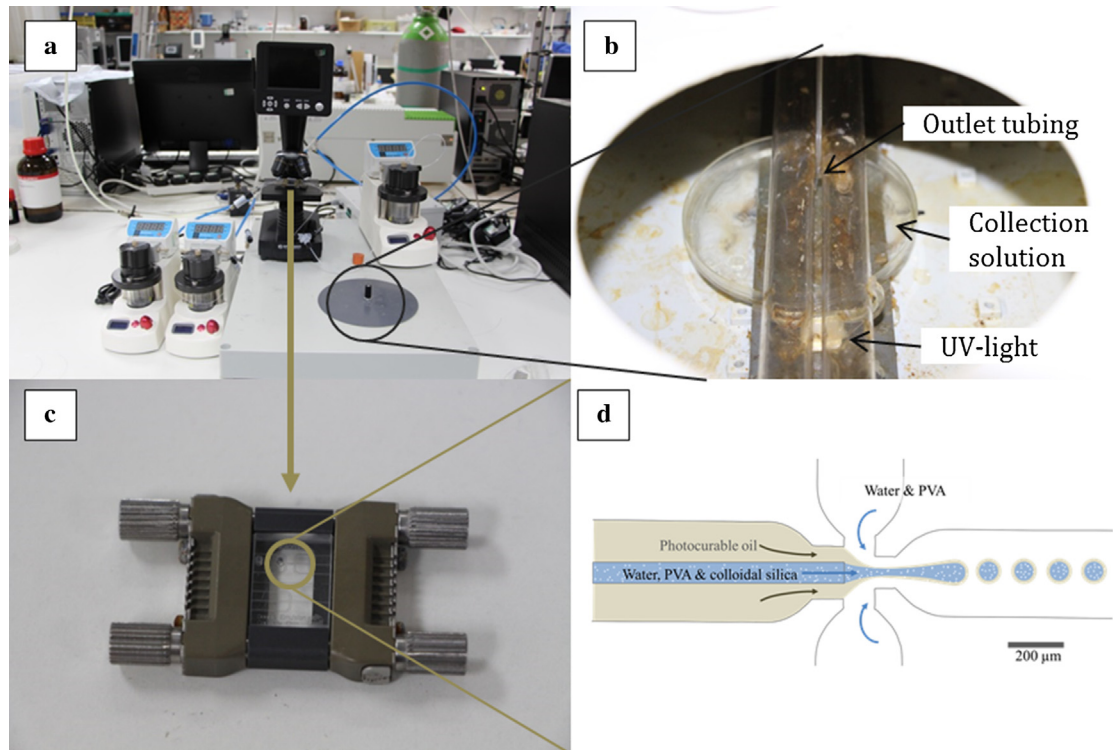
Fig. 2. The microfluidics platform used to produce the w/o/w double emulsion template (a) set-up used to produce microcapsules; (b) outlet of the collection tube where the double emulsion is photopolymerised; (c) microfluidic device and (d) schematic illustration of the formation of double emulsion template [33].

to minimise the effect of the density mismatch between the core and shell material [34]. The resultant microcapsules were collected in an aqueous solution of 10 wt% PVA solution to prevent the agglomeration of the microcapsules during the polymerisation.

2.2. Characterisation studies

The produced double emulsions were observed with an optical microscope (OM) (DM 2700 M, Leica, Germany) and the microcapsules' formation was confirmed with a scanning electronic microscope (SEM, Pro G2, Phenom, Netherlands). To obtain the capsules dimensions, the diameter was measured using the optical microscope and the shell thickness was measured using SEM. To do so, the microcapsules with oil core were ruptured between two glass slides, washed with ethanol to remove the mineral oil, and vacuum dried. The microcapsules with aqueous core were dried at room temperature for 1 day and then cut with a razor blade on the SEM stubs. To assess the thermal stability and oil content, the microcapsules were dried for 2 days before the thermogravimetric analysis (TGA) using PerkinElmer STA6000 between 50 and 700 °C at a rate of 5 °C/min, under air atmosphere. For investigation of the colloidal silica content, the microcapsules were ruptured with a razor blade in a SEM stub and the SEM-EDX analysis was performed using a Nova nanoSEM 450 equipped with a Bruker Quantax Xflash 6/100 EDX detector under a 10 kV accelerating voltage.

To investigate the integration and the mechanical triggering of the microcapsules, cement paste prisms (10 × 10 × 100 mm) were produced by hand-mixing ordinary Portland cement (CEMI 52.5N) with a water-to-cement ratio of 0.45 and 3 wt% of microcapsules with respect to the cement mass. For the investigation of mechanical triggering, the microcapsules with BH shell, the colloidal silica (CS) as core and the outer diameter of 88 μm and shell thickness of 7 μm (labeled BH-88/7) were used as example of the aqueous core; alternatively, microcapsules with BI shell, mineral oil as core and the outer diameter of 110 μm and shell thickness of 2 μm (labeled BIMO-110/2) were investigated as example of organic core. For the investigation of the interfacial bonding, the microcapsules with aqueous core were BHA-195/15 and BIAMO-110/2 was an example of organic core. After 24 h of casting, the prisms were demolded, a small portion was fractured and the specimen was dried under vacuum for 2 h for SEM observation. The sample BH-88/7 was submerged for further hydration and SEM observations took place at 1, 14 and 64 days, as observed in Fig. 7a, b and c, respectively.

The microcapsules and acrylates were mechanically characterised by means of Dynamic Mechanical Analysis (DMA) and microindentation. DMA measurements were performed on a DMA 8000 apparatus (PerkinElmer) operated in tension mode. To prepare the samples, 1 mL of each acrylate solution was poured in a plastic petri

dish and covered with 4 mL of PVA 10% solution to avoid the intrusion of oxygen and to disperse the heat of the exothermic polymerisation reaction. The solution was placed above a UV-lamp for 5 min. Once the material was polymerised, the acrylate sheet was demoulded, and washed with ethanol to remove reminiscent PVA and unreacted acrylates. The samples were carefully cut with a razor blade at orthogonal shapes with dimensions 25 × 6.5 × 0.3 mm. This procedure was carried out shortly after the polymerisation to prevent the formation of small cracks during cutting. During the analysis, the sample was placed in a dual cantilever jig and subjected to a frequency of 1 Hz at a heating rate of 5 °C min^{-1} from −50 to 120 °C. In this way, the storage modulus (E′), loss modulus (E″) and loss factor (tan δ) were calculated; the glass transition temperature was considered based on tan δ peak.
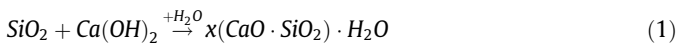
For the microindentation, the specimens were prepared by pouring 4 mL of each acrylate solution (BI and BH) in a cylindrical transparent mold and covering the acrylate with 10 mL of PVA 10 wt%. The cylinder was then placed above a UV-lamp for 10 min, followed by 20 min of lateral exposure. The formed polyacrylate disc was washed with ethanol and the meniscus formed at the bottom of the sample removed using a disc cutter (Presi Mecatome T255/300). To obtain a smooth surface for the indentation, the top surface was carefully wet ground with 1200, 2500 and 4000 grit SiC paper (MetPrep), followed by final polishing using 0.3 μm alumina suspension (MetPrep) on a Mecapol P225 (Presi). The resultant disc was 32 mm diameter and 10 mm thickness and the indentation was performed on the polished top surface one day after the polymerisation. The instrumented indentation platform (MHT, Anton Paar) was used with a Vickers diamond indenter with the elastic modulus of 1141 GPa and the Poisson's ratio of 0.07; the Poisson's ratio of the acrylates was considered 0.35 [35]. The samples were loaded at a rate of 400 mN min^{-1} until a peak of 1000 mN when the maximum load was kept constant for 20 s and then the samples were unloaded at the same rate. For each sample, at least 15 indentations were performed at different points on the surface. Instrumented indentation was also used to measure the Young's modulus of single microcapsules. To do so, the microcapsules were carefully dispersed over a steel stub coated with a thin layer of glue. A flat punch indenter (200 μm diameter) was used to obtain the load-displacement curve used for the calculation of the Young's modulus. Three microcapsules were loaded at a rate of 30 mN min^{-1} until a peak of 30 mN when the load was kept constant for 10 s and then the samples were unloaded at the same rate.

Tensile strength and elongation at break of the acrylate samples were directly measured with an INSTRON frame (model 1011). The samples were prepared in a similar protocol used for the DMA, and then cut into small plaques (8 × 0.4 mm) to perform tensile tests. The tests were performed with maximum load of 250 N, crosshead speed of 1 mm min^{-1} and the gauge length was 20 mm. The tests were carried out at 20 ± 2 °C.

3. Results and discussion

3.1. Preparation of monodisperse aqueous core microcapsules

A flow-focusing device was used to produce monodisperse w/o/w double emulsion droplets which served as a template for the formation of microcapsules. The device consisted of a fluorophilic coated capillary placed before a hydrophilic flow focusing droplet junction, which enabled the formation of water-in-oil-in-water droplets (w/o/w) (Fig. 2c). The monodisperse double emulsion template (Fig. 3a) was comprised of a 50 wt% 1,6-hexanediol diacrylate and 50 wt% bisphenol A glycerolate dimethacrylate solution termed BH as middle phase. The inner phase consisted of an aqueous solution containing colloidal silica (CS) and PVA. After the polymerisation of the photocurable oil, optical microscope (Fig. 3b) and SEM images revealed the core–shell structure containing the colloidal silica within (Fig. 3c, d). The capsules were labelled BHCS-88/9 due to their BH shell, CS core, 88 μm outer diameter and 9 μm shell thickness. Both the size and shell thickness of the microcapsule can be tuned by changing the flow rates of the different phases [29]; however, due to the stability of the w/o/w double emulsion, the minimum shell thickness obtained was 7 μm. The presence of CS as core had a twofold purpose. Firstly, nano-SiO$_2$ particles could interact chemically with the calcium hydroxide present in a cementitious matrix, as part of the cement hydration process, leading to the formation of Calcium Silicate Hydrate gel (CSH) (Eq. (1)).

$$SiO_2 + Ca(OH)_2 \overset{+H_2O}{\rightarrow} x(CaO \cdot SiO_2) \cdot H_2O \qquad (1)$$

This process is known to enhance the mechanical and durability properties and more recently was reported to promote self-healing in cement-based mortars [36]. Secondly, CS increases the density of the inner aqueous phase and thus minimises the density mismatch between the inner and middle phases [34], favouring the formation of spatially homogenous shells.

The aqueous core was investigated because water plays a key role in the biological and mineral self-healing of cement-based materials [37]. In both cases, water is necessary for promoting the chemical reactions between the healing agent and the host cementitious matrix. Additionally, in the encapsulated systems, water acts as the dispersant medium of the healing compound [38,39]. Dispersing the healing agent into a liquid will result in its higher mobility, compared to encapsulated solid particles, thus covering a larger surface area of the damage location. However, the acrylate shell is permeable to water, while impermeable to ions and molecules with high molecular weight [29,40]. In general, the permeability depends on the degree of crosslinking and the polarity of the core and the shell material, but water can permeate even through the crosslinkable perfluorinated membranes under osmotic stress [30]. Thus, the water encapsulated as core material evaporated through the shell, leaving the CS and the PVA within the microcapsules. The presence of CS was confirmed by SEM which showed the white powder inside the shell (Fig. 3c) and EDX scans of the fractured microcapsules. As shown in Fig. 4, at point 1, localised inside of a cut microcapsule, the signal of silicon, oxygen and carbon are clearly visible and indicate the presence of CS inside the microcapsule. Alternatively, at point 6 where only the shell material is analysed, only a carbon peak and a weaker signal of oxygen
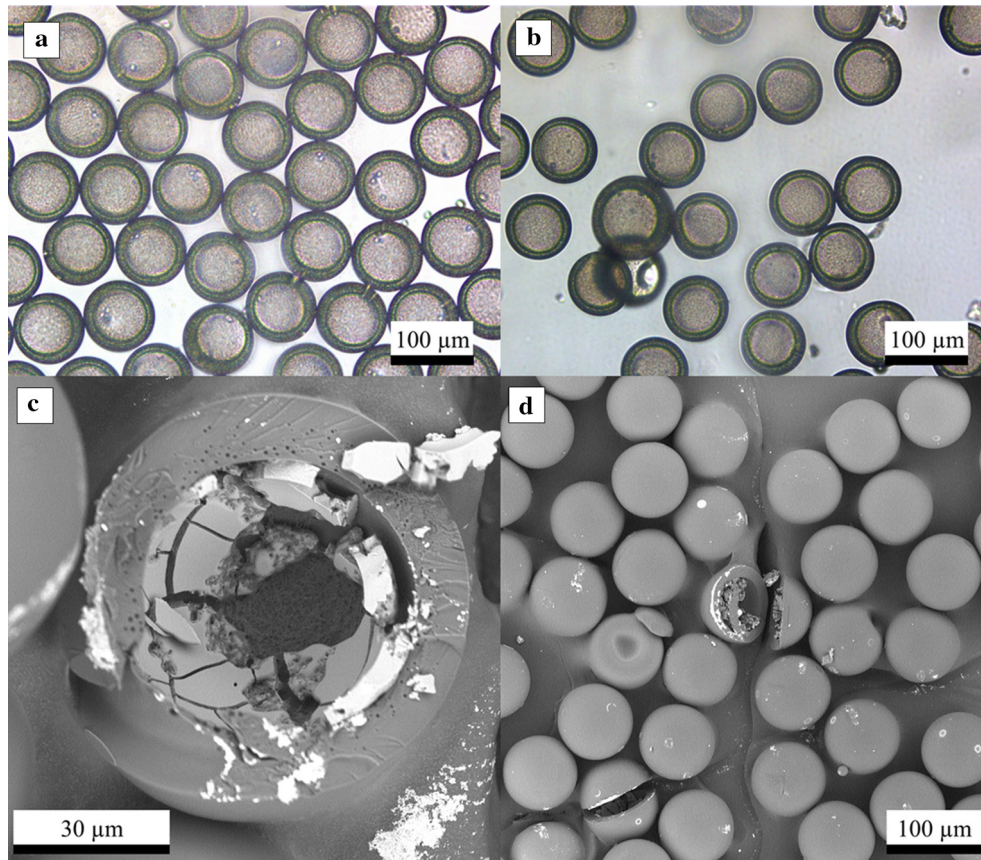

Fig. 3. Images of microcapsules BHCS-88/9 produced in the microfluidics device: (a) optical microscope image of the monodisperse double emulsion before photopolymerisation; (b) microcapsules in water after photopolymerisation; (c) a close-up of a ruptured microcapsules and (d) SEM images of the dried microcapsules with one visibly ruptured microcapsule.
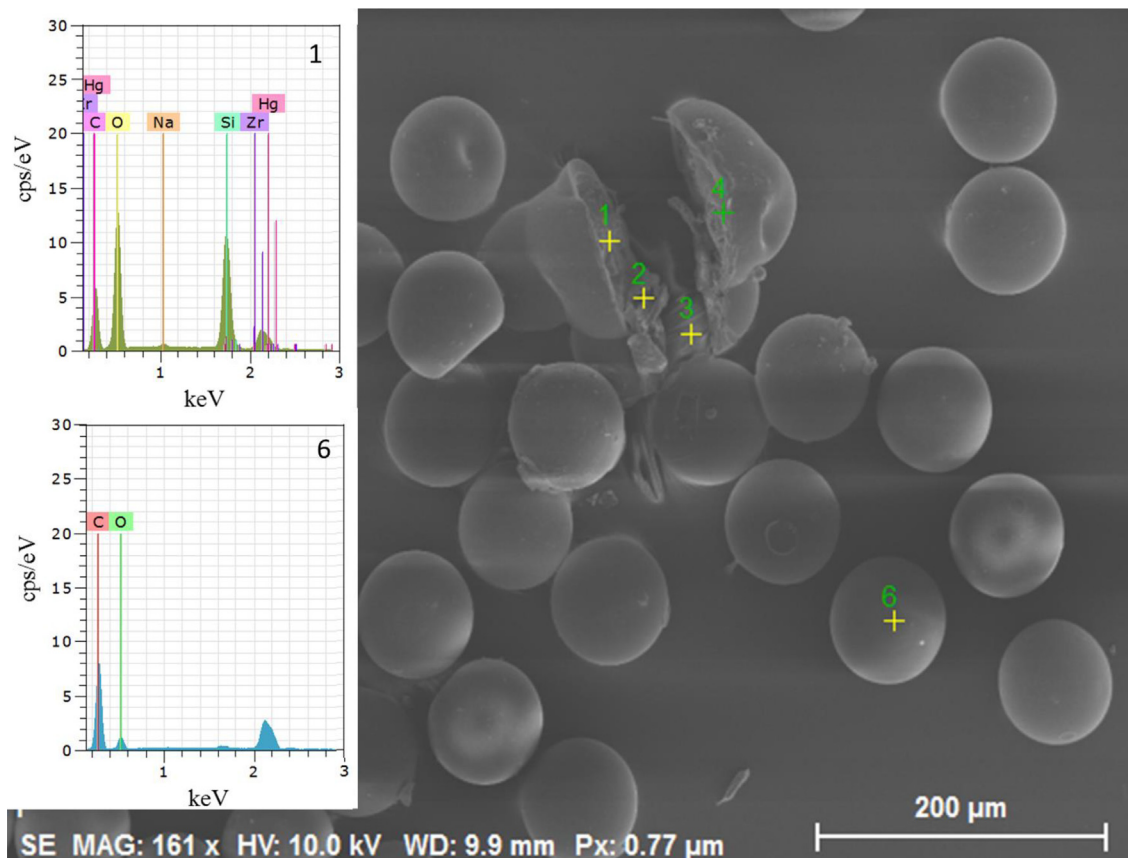
Fig. 4. SEM micrograph of the cut and non-cut microcapsules. On the left are the representative EDX spectra of point 1 (inside the microcapsule) and point 6 (microcapsule shell).

can be detected. Thus, the shells with 9 μm thickness were found to be water-permeable, resulting in the retention of only colloidal silica and PVA. Similar results were observed with polyurethane shells, where only solid sodium silicate was retained inside the microcapsule while the aqueous phase was lost [19]. Furthermore, with the decrease of shell thickness, the water-permeability increases. Thus, when capsule-based self-healing uses liquid healing agent, a more efficient approach is to encapsulate non-aqueous materials which are more likely to be retained inside of the shell [10,11,16].

3.2. Preparation of monodisperse non-aqueous core microcapsules

To produce microcapsules capable of retaining the liquid core, mineral oil was investigated as model organic core material. An oil-in-oil-in-water (o/o/w) double emulsion droplet was used as template for the formation of the microcapsules, as shown in Fig. 5a. To demonstrate the versatility of the device to produce microcapsules with different core and shell materials, a mixture of 50 wt% isobornyl acrylate and 50 wt% bisphenol A glycerolate dimethacrylate solution labelled BI was used as middle phase. Then, the microcapsules were obtained (Fig. 5b) by cross-linking the photocurable oil phase in the double emulsion drops at the exit of the collection tube. The obtained microcapsules (Fig. 5c and d) were named BIMO-110/2 due to the BI shell, the mineral oil (MO) as core, the outer diameter of 110 μm and shell thickness of 2 μm. Due to decreased interfacial tension between the inner and middle phase in an o/o/w double emulsion, the template is more stable and allows the production of microcapsules with decreased shell thicknesses. Furthermore, the thinner shell increases the payload of the microcapsules, thus maximising the amount of core material and healing agent.

The retention of mineral oil inside of the microcapsules was demonstrated by the thermogravimetric analysis (TGA) of the microcapsules BIMO-110/2, as shown in Fig. 6. The thermal degradation of neat mineral oil under air atmosphere takes place between 150 and 300 °C, as observed in the red line of Fig. 6. On the other hand, the decomposition curve of the bulk sample of the acrylate shell (grey line) is not complete before 500 °C. For the microcapsules at 400 °C, all the oil is likely to be decomposed while the shell is still present. Thus, by contrasting the decomposition curve of the microcapsules (black line) with the shell (grey line) at 400 °C, the shell material was calculated to be 43%. Furthermore, the mass balance of 57% was attributed to mineral oil as core. Based on the diameter and shell thickness of the double emulsion (110 and 2 μm, respectively), the expected core-to-shell volume ratio is 8.5:1, which corresponds to a theoretical weight fraction of mineral oil of 87% relative to the total capsule mass. Thus, the estimated encapsulation efficiency is 66% relative to the original mineral oil engulfed in the double emulsion. The loss of mineral oil can be attributed to the effects of gravitational settling due to the density mismatch of the mineral oil and acrylate phases. This led to the formation of spatially inhomogeneous emulsions and the escape of the mineral oil during polymerisation, consequently reducing the encapsulation efficiency [33,41]. However, the dispersion of healing agent to the organic carrier phase can increase the density of the inner phase and thus minimise the density mismatch and increase the encapsulation efficiency.

3.3. Mechanical triggering of the microcapsules for self-healing

To investigate their survivability and mechanical triggering, microcapsules containing aqueous and organic core were embedded in the cementitious matrix. To assure the healing agent is
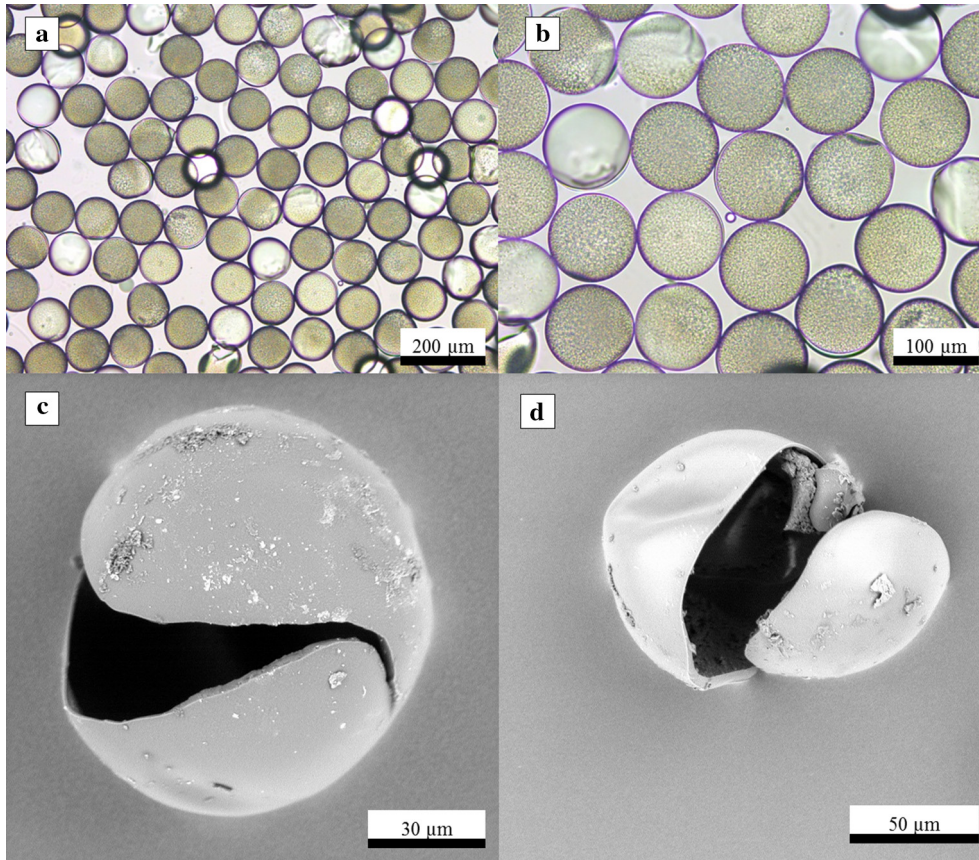
Fig. 5. Microcapsules BIMO-110/2. Optical microscope images of (a) the monodisperse double emulsion before polymerisation and the (b) microcapsules after polymerisation; (c) and (d) SEM images of the dried and ruptured microcapsules without mineral oil.
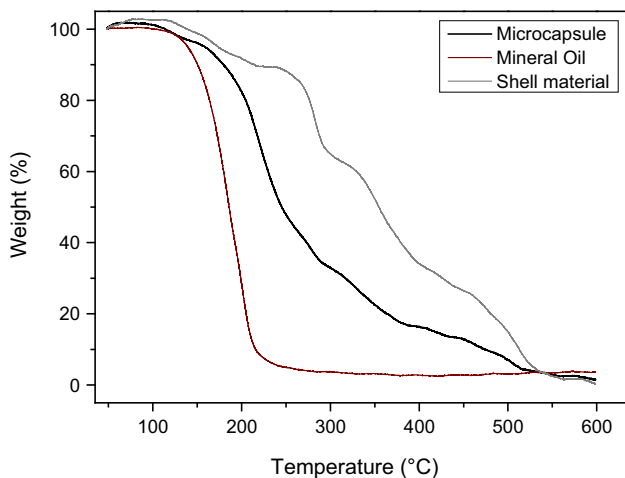

Fig. 6. TGA curves of dried BIMO-110/2 microcapsules (black line), the bulk shell material (grey line) and the mineral oil (red line). (For interpretation of the references to colour in this figure legend, the reader is referred to the web version of this article.)

released upon crack formation, the microcapsules need to survive the mixing and be mechanically triggered by crack. However, the survival can be challenging, due to the strong alkalinity of cementitious matrices (pH > 12), the high shear during mixing and elevated temperatures ranging from 35 to 80 °C during the cement hydration and setting processes. Nonetheless, in this case SEM images revealed that the microcapsules with the acrylate shell

survived mixing and exposure in the alkaline cementitious environment, as shown in Fig. 7. In an opposite scenario, the microcapsules would have not retained their characteristic spherical shape and excessive amount of ruptured shells and debris would have been observed.

To observe the mechanical triggering of microcapsules with aqueous core microcapsules, the sample BH-88/7 was used with BH shell, aqueous core, 88 μm outer diameter and 7 μm shell thickness. When the cement paste prisms were fractured, it was observed that, although some water core microcapsules were broken (Fig. 7a), most of them remained unbroken upon crack. This behavior was partially attributed to the loss of encapsulated water leading to deformation of its original spherical shape due to an evaporation-induced pressure decrease [34,40]. During hydration and hardening of the cement paste, the buckling and collapsing of the shell led to the formation of dimples, as observed from the cavity shapes in Fig. 7b and c. Microcapsules with thicker shell could be produced, slowing down the process of water loss through the shell and maintaining the capsule spherical shape after the evaporation of water [40]. However, the smaller core to shell ratio would decrease the payload of healing agent and increase the residual footprint of the shell. Additionally, a thicker shell precludes the mechanical triggering of the microcapsule. While aqueous core microcapsules rarely show broken shells, ruptured organic core microcapsules were observed after just 1 day of casting, as shown in Fig. 7d and e. In this case, the microcapsules were BIMO-110/2 with BI shell, mineral oil as core, 110 μm outer diameter and 2 μm shell thickness. This difference hints the importance of thin shelled microcapsules to facilitate the ruptured upon crack. Also, the organic was retained inside of the shell, resulting in the
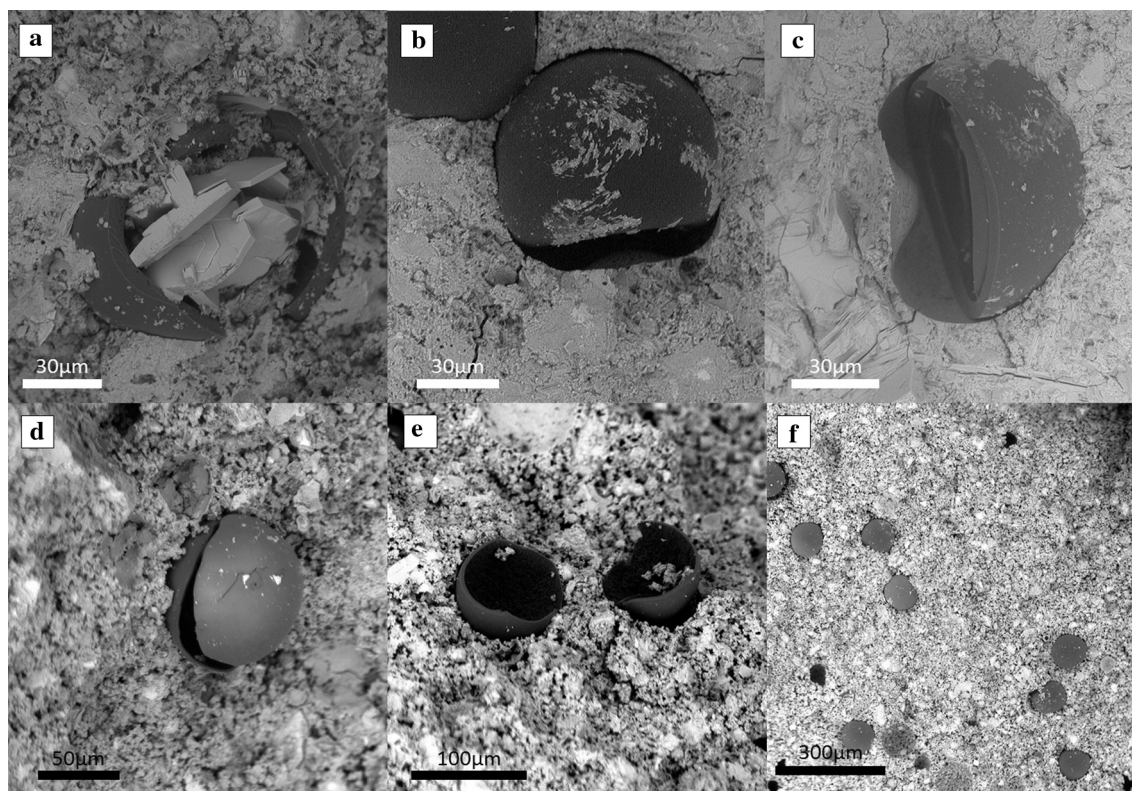
Fig. 7. Integration of microcapsules with aqueous (top) and organic core (bottom) in the cement paste. SEM images of broken (a) and unbroken (b, c) BH-88/7 microcapsules due to poor interfacial bonding, shrinkage and collapse; SEM images of broken (d, e) and (f) debonded BIMO-110/2 due to poor interfacial bonding.

maintenance of the spherical shape of the microcapsules and thus better contact between the shell and the matrix. However, due to the poor interfacial bonding, most of the microcapsules with organic core still debond without rupture as shown in Fig. 7f.

To successfully induce the mechanical triggering of the microcapsules, it is essential to achieve a good interfacial bonding between them and the cementitious matrix; otherwise, debonding may occur [20]. In the microfluidics technique, the interfacial tension that enables the formation of the w/o/w and o/o/w template results in microcapsules with a smooth hydrophobic shell surface. This results in a poor mechanical interlock and the formation of a non-cohesive layer between the microcapsules and the cementitious matrix. As a result, debonding is observed instead of cracking, as shown in Fig. 7. Previous microencapsulation and mechanical trigger investigation for self-healing revealed debonding for other polymeric shell materials such as urea-formaldehyde [15] and phenol-formaldehyde [17]. On the other hand, silica [26] and hydrophilic gelatin [11,18] have shown good interfacial bonding. Likewise, research has shown that the lack of chemical interaction between the hydrophobic fibers and the cementitious matrix results in poor bond strength [22]. Alternatively, the introduction of hydroxyl groups on the surface of hydrophilic fibers favored good interfacial bonding through the nucleation and growth of cement hydration products [23].

To improve the interfacial bonding between the shell and the matrix, the microcapsules were functionalised with hydrophilic groups and the process is illustrated in Fig. 8a. Acrylic acid was added to the outer aqueous PVA solution during the formation of the double emulsion template. During the photopolymerisation of the acrylate shell, the radicals also initiated the polymerisation of the acrylic acid in the surrounding solution, attaching a chain of carboxyl groups to the surface of the microcapsule. The process appeared to be efficient on consuming most of the acrylic acid,

since its distinct acrid odour was not noticed in the collecting solution.

To investigate the effect of the surface modification on the matrix-microcapsule interlock, microcapsules, with aqueous and organic cores, functionalized with polar hydroxyl groups were embedded in the cement paste. The acid dissociation logarithmic constant (pK_a) of the acrylic acid is 4.2, consequently the polymer is deprotonated in the alkaline environment of the cement paste. The carboxylate ion attracts cations from the paste, e.g., Ca^{2+} or Na^+, thus improving the bond with the cementitious matrix [42]. The results of the improved bond are shown in Fig. 8. The microcapsules are clearly covered by a layer of hydration products (Fig. 8b–d) as opposed to smooth microcapsules without functionalisation (Fig. 7a–f). This indicates the facilitated nucleation of cement hydration products on the outer surface of the hydrophilic shell. These nucleation sites provide cohesion with the surrounding cementitious matrix improving the mechanical interlock of the microcapsules. Nonetheless, although the interfacial bonding improved, the shrinkage and collapse of the microcapsules having aqueous core still hinder the fracture upon crack formation [33]. On the other hand, the microcapsules with oil-core were mostly broken when crack formed, as shown in Fig. 8e–g. In this case, the microcapsules maintained the spherical shape, presented thinner shells and formed strong adhesion to the surrounding matrix facilitated their fracture and the subsequent release of the cargo material.

3.4. Mechanical properties of the acrylate shell

The glass transition temperature, Young's Modulus and tensile strength of the acrylates used to form the microcapsules' shells were quantified and are shown in Table 1. The aim was to take advantage of the versatility of the double emulsion template to
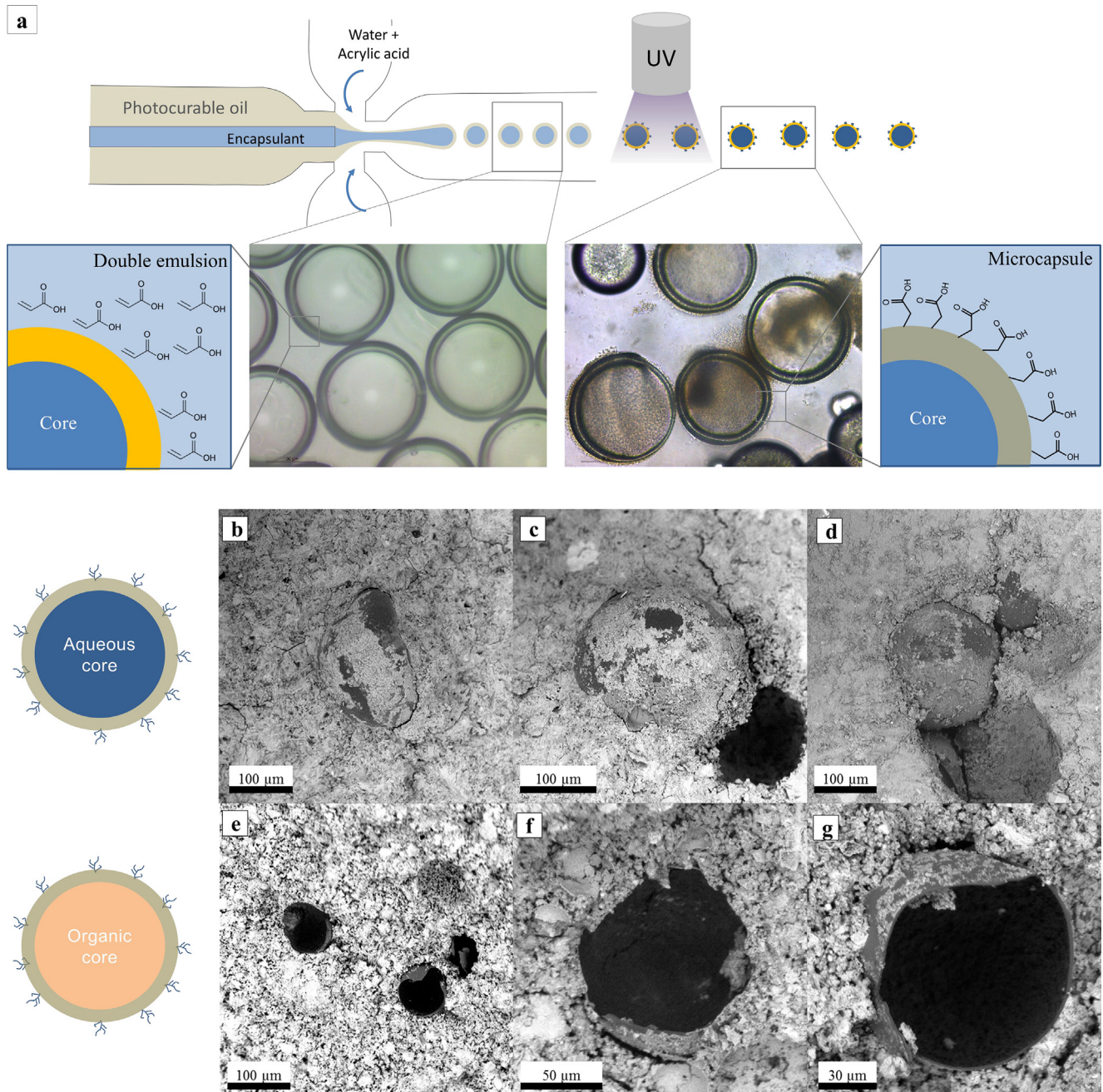
Fig. 8. Encapsulation of aqueous and non-aqueous cargo material and with the surface functionalised with poly(acrylic acid). (a) Schematic illustration of the microfluidic device used for the production of the double emulsion template and the photopolymerisation process; SEM images of aqueous (b–d) and non-aqueous (e–g) microcapsules integrated in the cement paste.

tune the mechanical properties of the acrylates to maximise the mechanical triggering of the microcapsules. In this sense, the mismatch of properties between the host matrix and the microcapsules is crucial, particularly the elastic modulus, fracture toughness/strength and interfacial bond strength [20]. The measured glass transition temperature (T_g) of the copolymer was 43 and 86 °C, for BH and BI, respectively, as shown in Table 1. The sample BI presented the higher T_g due to the presence of bulky isobornyl side groups attached to the polymer backbone, which restrict the molecular rotation. The tuning of the glass transition to range between 40 and 60 °C is desirable as it can result in ductile shell during the exothermic mixing/setting of the cementitious composite and in a more brittle material after the hardening when the temperature drops [43]. Therefore, BH formed shells more duc-

Table 1
Glass transition and mechanical properties of the acrylate used in the microcapsules shell.

Sample	T_g/°C	Young's modulus/GPa	Tensile strength/MPa
BH	43	2.6 ± 0.2	35.2 ± 4.6
BI	86	2.4 ± 0.2	14.8 ± 0.03

tile and hence more likely to survive mixing. In contrast, BI formed brittle shells more likely to rupture under crack and release the core material, as shown in the Fig. 7d–f and Fig. 8e–g. However, it also increases the likelihood of broken microcapsules due to the high shear during mixing.
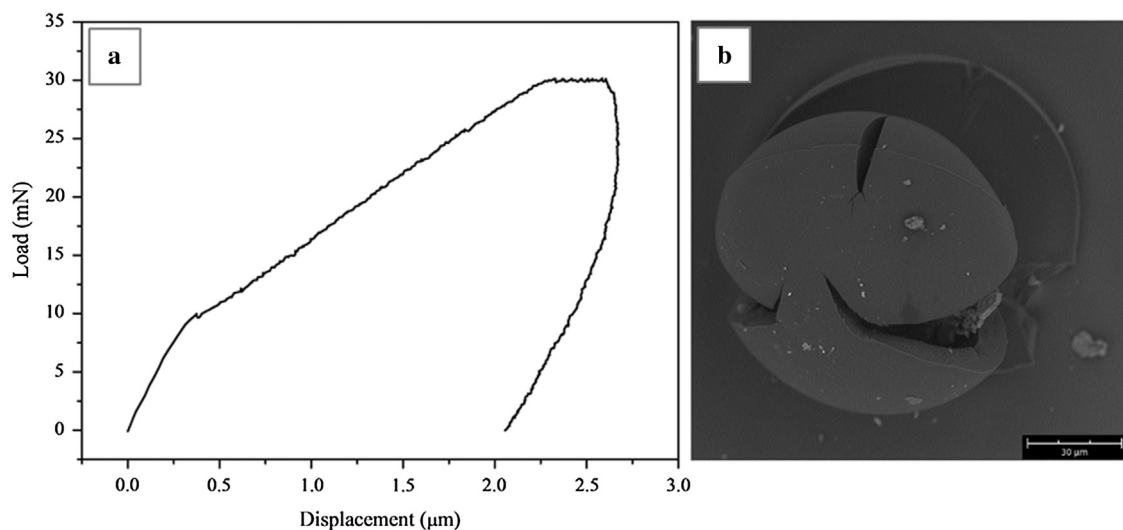
Fig. 9. (a) Typical load-displacement curve of BHCS-88/9 capsules and (b) SEM image showing the fracture of the microcapsules after the indentation at maximum load of 30mN.

To determine the effect of shell materials in the elastic modulus of the microcapsules, the Young's modulus of the copolymers was measured using instrumented indentation. The values of Young's modulus obtained for copolymers BI and BH were 2.4 and 2.6 GPa, respectively, as shown in Table 1. The presence of phenyl hydrogens in the bisphenol results in a steric hindrance and a rigid structure is expected, increasing the elastic modulus of the copolymers. The elastic modulus of the individual microcapsules was also measured using the flat punch indenter. A typical example of the indentation curve and a example of a damaged microcapsule is shown in Fig. 9. The Young's modulus of microcapsules BHCS-88/9 was 2.6 ± 0.8 GPa; this value was the same as the bulky material, but differences due to the size and shell thickness of the microcapsules are expected [17]. These values are lower than the elastic modulus of concrete, typically ranging between 20 and 38 GPa. Thus, given a good interfacial bonding between the matrix and the microcapsules, this mismatch favours the mechanical triggering of the microcapsules, since a less stiff inclusion will create a preferential path for the formed crack [20]. However, the insertion of the microcapsules with reduced values of Young's modulus, compared with the matrix, is likely to reduce the overall elastic modulus of the matrix [11].

The tensile tests were conducted at room temperature, which is below the glass transition temperature of the copolymers and thus a complete brittle fracture took place. The copolymers presented a stress at rupture of 15 and 36 MPa, and strain values of 5.3 and 9.7%, for BI and BH, respectively. The copolymer BH presented the highest value of stress and strain and certain toughening process, which can be related with the lower T_g of BH. The combination of higher toughness, tensile strength of 36 MPa and thicker shell may have precluded the shell fracture for the BH microcapsules. Alternatively, given a good interfacial bonding, the brittle BI microcapsules with shell thickness of 2 μm were mechanically triggered despite the tensile strength of 15 MPa being higher than the matrix (tensile strength of concrete ~2–5 MPa).

4. Conclusions

For the first time, a microfluidic device was used to produce microcapsules containing aqueous and organic core material applied for self-healing in cementitious materials. The w/o/w double emulsion template was formed and UV-polymerised to form the core-shell structure using colloidal silica and water as core. Although water was encapsulated, it evaporated through the nano-pores of the shell, leaving the colloidal silica inside the microcapsules. The o/o/w template was used for the production of microcapsules with mineral oil, rendering an encapsulation efficiency of 66%. The organic core is preferable for self-healing since it is retained inside the polymeric shell and can be used as delivery vehicle for the healing agent. When assessing the mechanical triggering, the aqueous core microcapsules presented a thicker shell which precluded the rupture upon crack. Moreover, these microcapsules buckled and collapsed due to the loss of water during the hydration of the cement paste. Alternatively, organic core microcapsules have a thinner shell, and retained the core, thus maintaining the spherical shape. However, due to the poor interfacial bonding between the hydrophobic shell and the cement matrix, the microcapsules debonded without rupture. To improve the interfacial bonding between the microcapsules and the matrix, the shell was functionalised with hydrophilic groups, enhancing the bonding with the cement paste. As a result, the microcapsules containing organic core and functionalised shell were physically triggered upon crack formation. Investigation on the mechanical properties of the microcapsules indicated that the Young's modulus is lower than the one of concrete, which favors the mechanical triggering. Moreover, the use of shell with a high T_g and low tensile strength facilitated the triggering of the microcapsules. Thus, the key factors governing mechanical triggering were tuned to enhance the rupture of the capsule and promote self-healing, namely: (i) good interfacial bonding; (ii) thin shelled microcapsules; (iii) the retention of the core material; and (iv) low fracture toughness and strength.

The approach outlined in this work can be further extended to encapsulate most the typical healing agents used for self-healing in cementitious materials. Moreover, our strategy to functionalise the surface of the microcapsule to increase the interfacial bonding enhances the types of the shell that can be used for mechanical triggering. This opens up new opportunities for a wider range of shells and core materials to be investigated to promote self-healing.

Conflict of interest

None.

Acknowledgements

References

[1] Office for National Statistics, Construction Statistics Annual Tables, (2016). https://www.ons.gov.uk/businessindustryandtrade/constructionindustry/datasets/constructionstatisticsannualtables (Accessed 16 June 2017).

[2] P.H. Emmons, D.J. Sordyl, The state of the concrete repair industry, and a vision for its future, Concr. Repair Bull. (2006) 7–14. Accessed 21 December 2016.

[3] NACE International, Corrosion Costs and Preventive Strategies In the United States, (n.d.) 12. https://www.nace.org/uploadedFiles/Publications/ccsupp.pdf (Accessed 16 June 2017).

[4] G.H. Koch, M. Brongers, N.G. Thompson, Y.P. Virmani, J.H. Payer, Corrosion cost and preventive strategies in the United States, 2002. https://trid.trb.org/view.aspx?id=707382 (Accessed 16 June 2017).

[5] C.L. Freyermuth, Life-cycle cost analysis for large bridges, Concr. Int. 23 (2001) 89–95. Accessed 12 July 2017.

[6] K. van Breugel, Is there a market for self-healing cement based materials? in: Proc. First Int. Conf. Self Heal. Mater., Noordwijk aan Zee, The Netherlands, 2007. file:///C:/Users/lrds2/Downloads/documents-82.pdf.

[7] K. Van Tittelboom, N. De Belie, Self-healing in cementitious materials—a review, Materials (Basel). 6 (2013) 2182–2217, https://doi.org/10.3390/ma6062182.

[8] N. De Belie, E. Gruyaert, A. Al-Tabbaa, P. Antonaci, C. Baera, D. Bajare, A. Darquennes, R. Davies, L. Ferrara, T. Jefferson, C. Litina, B. Miljevic, A. Otlewska, J. Ranogajec, M. Roig-Flores, K. Paine, P. Lukowski, P. Serna, J.-M. Tulliani, S. Vucetic, J. Wang, H.M. Jonkers, A review of self-healing concrete for damage management of structures, Adv. Mater. Interfaces (2018), https://doi.org/10.1002/admi.201800074.

[9] S. van der Zwaag, An Introduction to Material Design Principles: Damage Prevention versus Damage Management, in: S. van der Zwaag (Ed.), Self-Healing Mater., 2007: pp. 1–18. doi:10.1007/978-1-4020-6250-6_1.

[10] J.Y. Wang, H. Soens, W. Verstraete, N. De Belie, Self-healing concrete by use of microencapsulated bacterial spores, Cem. Concr. Res. 56 (2014) 139–152, https://doi.org/10.1016/j.cemconres.2013.11.009.

[11] P. Giannaros, A. Kanellopoulos, A. Al-Tabbaa, Sealing of cracks in cement using microencapsulated sodium silicate, Smart Mater. Struct. 25 (2016), https://doi.org/10.1088/0964-1726/25/8/084005 084005.

[12] A. Kanellopoulos, P. Giannaros, D. Palmer, A. Kerr, A. Al-Tabbaa, Polymeric microcapsules with switchable mechanical properties for self-healing concrete: synthesis, characterisation and proof of concept, Smart Mater. Struct. 26 (2017), https://doi.org/10.1088/1361-665X/aa516c 045025.

[13] M.M. Hassan, J. Milla, T. Rupnow, M. Al-Ansari, W.H. Daly, Microencapsulation of calcium nitrate for concrete applications, Transp. Res. Rec. J. Transp. Res. Board 2577 (2016) 8–16, https://doi.org/10.3141/2577-02.

[14] L. Lv, Z. Yang, G. Chen, G. Zhu, N. Han, E. Schlangen, F. Xing, Synthesis and characterization of a new polymeric microcapsule and feasibility investigation in self-healing cementitious materials, Constr. Build. Mater. 105 (2016) 487–495, https://doi.org/10.1016/j.conbuildmat.2015.12.185.

[15] X. Wang, F. Xing, M. Zhang, N. Han, Z. Qian, Experimental study on cementitious composites embedded with organic microcapsules, Materials (Basel). 6 (2013) 4064–4081, https://doi.org/10.3390/ma6094064.

[16] G. Perez, E. Erkizia, J.J. Gaitero, I. Kaltzakorta, I. Jiménez, A. Guerrero, Synthesis and characterization of epoxy encapsulating silica microcapsules and amine functionalized silica nanoparticles for development of an innovative self-healing concrete, Mater. Chem. Phys. 165 (2015) 39–48, https://doi.org/10.1016/j.matchemphys.2015.08.047.

[17] L. Lv, E. Schlangen, Z. Yang, F. Xing, Micromechanical properties of a new polymeric microcapsule for self-healing cementitious materials, Materials (Basel). 9 (2016) 1025, https://doi.org/10.3390/ma9121025.

[18] A. Kanellopoulos, P. Giannaros, A. Al-Tabbaa, The effect of varying volume fraction of microcapsules on fresh, mechanical and self-healing properties of mortars, Constr. Build. Mater. 122 (2016) 577–593, https://doi.org/10.1016/j.conbuildmat.2016.06.119.

[19] A. Beglarigale, Y. Seki, N.Y. Demir, H. Yazıcı, Sodium silicate/polyurethane microcapsules used for self-healing in cementitious materials: monomer optimization, characterization, and fracture behavior, Constr. Build. Mater. 162 (2018) 57–64, https://doi.org/10.1016/j.conbuildmat.2017.11.164.

[20] S.A. Ponnusami, S. Turteltaub, S. Van Der Zwaag, S. van der Zwaag, Cohesive-zone modelling of crack nucleation and propagation in particulate composites,

[21] Eng. Fract. Mech. 149 (2015) 1–25, https://doi.org/10.1016/j.engfracmech.2015.09.050.

[21] V. Li, C. Wu, S. Wang, A. Ogawa, T. Saito, Interface tailoring for strain-hardening polyvinyl alcohol-engineered cementitious composite (PVA-ECC), ACI Mater. J. (2002) 463–472.

[22] A. Peled, E. Zaguri, G. Marom, Bonding characteristics of multifilament polymer yarns and cement matrices, Compos. Part A Appl. Sci. Manuf. 39 (2008) 930–939, https://doi.org/10.1016/j.compositesa.2008.03.012.

[23] H.R. Pakravan, M. Jamshidi, M. Latifi, F. Pacheco-Torgal, Evaluation of adhesion in polymeric fibre reinforced cementitious composites, Int. J. Adhes. Adhes. 32 (2012) 53–60, https://doi.org/10.1016/j.ijadhadh.2011.08.009.

[24] M. Halvaei, M. Jamshidi, M. Latifi, Investigation on pullout behavior of different polymeric fibers from fine aggregates concrete, J. Ind. Text. 45 (2014) 995–1008, https://doi.org/10.1177/1528083714551437.

[25] E.N. Brown, M.R. Kessler, N.R. Sottos, S.R. White, In situ poly(urea-formaldehyde) microencapsulation of dicyclopentadiene, J. Microencapsul. 20 (2003) 719–730, https://doi.org/10.3109/02652040309178083.

[26] G. Perez, J.J.J. Gaitero, E. Erkizia, I. Jimenez, A. Guerrero, Characterisation of cement pastes with innovative self-healing system based in epoxy-amine adhesive, Cem. Concr. Compos. 60 (2015) 55–64, https://doi.org/10.1016/j.cemconcomp.2015.03.010.

[27] P.W. Chen, G. Cadisch, A.R. Studart, Encapsulation of aliphatic amines using microfluidics, Langmuir 30 (2014) 2346–2350, https://doi.org/10.1021/la500037d.

[28] A.S. Utada, E. Lorenceau, D.R. Link, P.D. Kaplan, H.A. Stone, D.A. Weitz, Monodisperse double emulsions generated from a microcapillary device, Science 308 (2005) 537–541, https://doi.org/10.1126/science.1109164.

[29] P.W. Chen, R.M. Erb, A.R. Studart, Designer polymer-based microcapsules made using microfluidics, Langmuir 28 (2012) 144–152, https://doi.org/10.1021/la203088u.

[30] M.A. Zieringer, N.J. Carroll, A. Abbaspourrad, S.A. Koehler, D.A. Weitz, Microcapsules for enhanced cargo retention and diversity, Small 11 (2015) 2903–2909, https://doi.org/10.1002/smll.201403175.

[31] Y.-J. Eun, A.S. Utada, M.F. Copeland, S. Takeuchi, D.B. Weibel, Encapsulating bacteria in agarose microparticles using microfluidics for high-throughput cell analysis and isolation, ACS Chem. Biol. 6 (2011) 260–266, https://doi.org/10.1021/cb100336p.

[32] J.J. Vericella, S.E. Baker, J.K. Stolaroff, E.B. Duoss, J.O. Hardin, J. Lewicki, E. Glogowski, W.C. Floyd, C.A. Valdez, W.L. Smith, J.H. Satcher, W.L. Bourcier, C.M. Spadaccini, J.A. Lewis, R.D. Aines, Encapsulated liquid sorbents for carbon dioxide capture, Nat. Commun. 6 (2015) 6124, https://doi.org/10.1038/ncomms7124.

[33] L.R. de Souza, Design and Synthesis of Microcapsules Using Microfluidics for Autonomic Self-Healing in Cementitious Materials (Doctoral thesis), University of Cambridge, 2017, https://doi.org/10.17863/CAM.16673.

[34] S.S. Datta, S.-H. Kim, J. Paulose, A. Abbaspourrad, D.R. Nelson, D.A. Weitz, Delayed buckling and guided folding of inhomogeneous capsules, Phys. Rev. Lett. 109 (2012) 134302, https://doi.org/10.1103/PhysRevLett.109.134302.

[35] P. Chen, J. Brignoli, A.R. Studart, Mechanics of thick-shell microcapsules made by microfluidics, Polymer (United Kingdom) 55 (2014) 6837–6843, https://doi.org/10.1016/j.polymer.2014.10.060.

[36] A. Kanellopoulos, T.S. Qureshi, A. Al-Tabbaa, Glass encapsulated minerals for self-healing in cement based composites, Constr. Build. Mater. 98 (2015) 780–791, https://doi.org/10.1016/j.conbuildmat.2015.08.127.

[37] H. Huang, G. Ye, C. Qian, E. Schlangen, Self-healing in cementitious materials: materials, methods and service conditions, Mater. Des. 92 (2016) 499–511, https://doi.org/10.1016/j.matdes.2015.12.091.

[38] T.S. Qureshi, A. Kanellopoulos, A. Al-Tabbaa, Encapsulation of expansive powder minerals within a concentric glass capsule system for self-healing concrete, Constr. Build. Mater. 121 (2016) 629–643, https://doi.org/10.1016/j.conbuildmat.2016.06.030.

[39] R. Alghamri, A. Kanellopoulos, A. Al-Tabbaa, Impregnation and encapsulation of lightweight aggregates for self-healing concrete, Constr. Build. Mater. 124 (2016) 910–921, https://doi.org/10.1016/j.conbuildmat.2016.07.143.

[40] S.-H. Kim, T.Y. Lee, S.S. Lee, Osmocapsules for direct measurement of osmotic strength, Small 10 (2014) 1155–1162, https://doi.org/10.1002/smll.201302296.

[41] L.R. Souza, A.A. Kanellopoulos, A. Al-Tabbaa, Synthesis and characterization of acrylate microcapsules using microfluidics for self-healing in cementitious materials, in: Proc. 5th Int. Conf. Self-Healing Mater., Durham, NC, USA, 2015. https://goo.gl/ijPRFC.

[42] D. Hernández-Cruz, C.W. Hargis, S. Bae, P.A. Itty, C. Meral, J. Dominowski, M.J. Radler, D.A. Kilcoyne, P.J.M. Monteiro, Multiscale characterization of chemical–mechanical interactions between polymer fibers and cementitious matrix, Cem. Concr. Compos. 48 (2014) 9–18. http://www.sciencedirect.com/science/article/pii/S0958946514000067.

[43] B. Hilloulin, K. Van Tittelboom, E. Gruyaert, N. De Belie, A. Loukili, Design of polymeric capsules for self-healing concrete, Cem. Concr. Compos. 55 (2015) 298–307, https://doi.org/10.1016/j.cemconcomp.2014.09.022.